Cell Reports
Physical Science

CellPress
OPEN ACCESS

Article

Chemical recycling of post-consumer polyester wastes using a tertiary amine organocatalyst

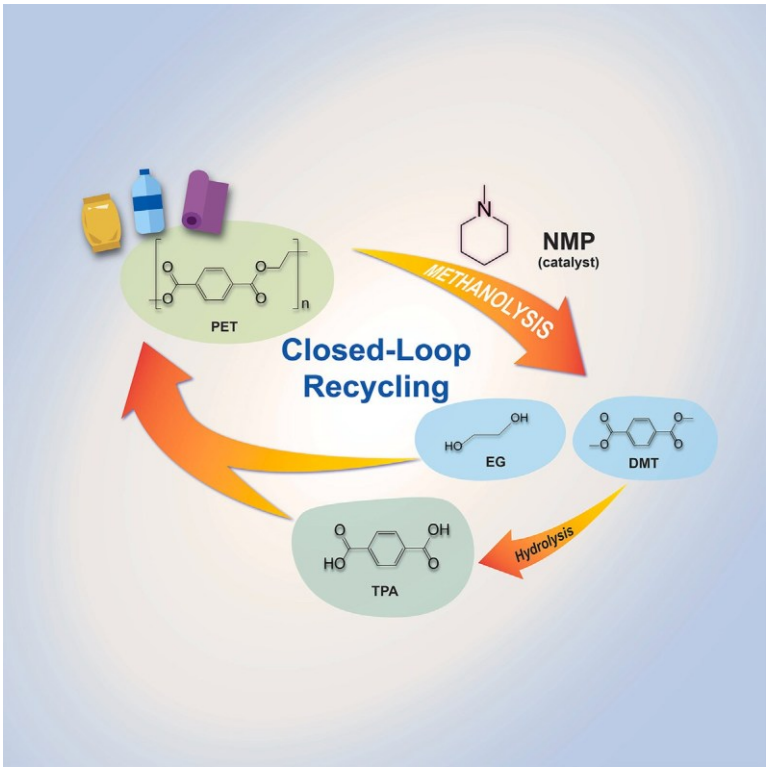

Plastic recycling is a promising yet challenging approach to addressing the accumulation of plastic pollution. Here, Xie et al. report a tertiary amine catalyst that selectively upcycles polyester into monomers or derivatives from waste plastic mixtures, providing an efficient chemical sorting strategy as an alternative to traditional mechanical recycling.

Shaoqu Xie, Caiqi Wang, Wenda Hu, ..., Nadia N. Intan, Jim Pfaendtner, Hongfei Lin

jianzhi.hu@pnnl.gov (J.Z.H.)
hongfei.lin@wsu.edu (H.L.)

Highlights

A series of amine catalysts are employed to depolymerize polyethylene terephthalate

The catalytic performance of various tertiary amines correlates with their basicity

A chemical sorting strategy is developed to recycle polyester from plastic waste

The decomposition mechanism is proposed based on NMR characterizations

Xie et al., Cell Reports Physical Science 5, 102145
August 21, 2024
https://doi.org/10.1016/j.xcrp.2024.102145

Cell Reports
Physical Science

CellPress
OPEN ACCESS

Article

Chemical recycling of post-consumer polyester wastes using a tertiary amine organocatalyst

Shaoqu Xie,[1,5] Caiqi Wang,[1,5] Wenda Hu,[1,2,5] Jian Zhi Hu,[1,2,*] Yong Wang,[1,2] Zhun Dong,[1] Nadia N. Intan,[3] Jim Pfaendtner,[3,6] and Hongfei Lin[1,4,7,*]

SUMMARY

Recycling diverse waste plastics poses challenges due to complex sorting and processing, resulting in high costs and inefficiency. To tackle this, we present a metal-free catalytic sorting method for targeted deconstruction of polyester from post-consumer plastic waste, encompassing textiles, plastic mixtures, and multilayer packaging materials. This method employs N-methylpiperidine, a tertiary amine catalyst in methanol, to depolymerize polyethylene terephthalate (PET). Operating under these conditions (160°C, 1 h), we achieve 100% yields of dimethyl terephthalate and ethylene glycol. This technique also effectively breaks down other polyesters, including polylactic acid, polycarbonate, and polybutylene terephthalate, yielding high-yield monomers at relatively low temperatures. Through comprehensive nuclear magnetic resonance (NMR) analysis, we propose that N-methylpiperidine's role is in enhancing methanol nucleophilicity and activating PET's ester bond. Our insights advance the chemical recycling of post-consumer plastic waste, offering a potentially simple and efficient path to closing the polyester production loop.

INTRODUCTION

Environmental concerns over accumulating plastic waste have heightened due to the enduring nature of most plastics, which can last in the environment for centuries.[1,2] Plastic recycling is vital for tackling this problem and facilitating the transition toward a circular economy and sustainable development. Various methods, such as mechanical recycling,[3] chemical recycling,[4] and biodegradation,[5,6] have been explored to achieve plastic recycling.

Mechanical recycling can lead to plastic downcycling or recombination into low-value products, primarily due to sorting limitations. Chemical recycling of plastic waste has gained attention, including processes like the tandem catalytic process by Scott et al. for polyethylene (PE) conversion to alkyl aromatics,[7] Hartwig et al.'s proposal of PE deconstruction into propylene,[8] and Huang et al.'s ultrasmall amorphous zirconia nanoparticles for polyolefin hydrogenolysis.[9] Our prior research showcased high-yield PE conversion to liquid fuel using the Ru/C catalyst.[10] Polyester chemical recycling approaches include hydrolysis,[11] alcoholysis,[12,13] glycolysis,[14–16] aminolysis,[17,18] and pyrolysis,[19,20] breaking down polyesters into monomers or value-added chemicals. Examples include polylactic acid upcycling catalyzed by quaternary ammonium fluoride,[21] aminolysis of polyesters with anilines catalyzed by lactate anion,[22] polylactic acid conversion into methyl methacrylate via a two-step catalytic process,[23] and polyethylene terephthalate (PET) and

[1]The Gene and Linda Voiland School of Chemical Engineering and Bioengineering, Washington State University, Pullman, WA 99164, USA

[2]Institute for Integrated Catalysis, Pacific Northwest National Laboratory, Richland, WA 99352, USA

[3]Department of Chemical Engineering, University of Washington, Seattle, WA 98195, USA

[4]Energy and Environment Directorate, Pacific Northwest National Laboratory, Richland, WA 99352, USA

[5]These authors contributed equally

[6]Present address: North Carolina State University, Raleigh, NC, USA

[7]Lead contact

*Correspondence: jianzhi.hu@pnnl.gov (J.Z.H.), hongfei.lin@wsu.edu (H.L.)

https://doi.org/10.1016/j.xcrp.2024.102145

polybutylene terephthalate (PBT) waste conversion using the $CuNa/SiO_2$ catalyst.[24] Notably, Niu et al.'s binuclear zinc catalyst enabled polyester depolymerization.[25] However, current methods often require clean plastic feedstock, and involve harsh conditions, costly catalysts, and low product yields. Thus, a robust, efficient chemical recycling approach is needed to process mixed plastic waste.

Polyesters, valued for their cost efficiency, versatility, and durability, have pervasive use in everyday life.[26] Among them, PET finds applications in textile fibers, bottles, and packaging.[27] While PET has undergone extensive mechanical recycling, this method tends to degrade rPET (recycled PET) quality, and rPET remains relatively costly compared to producing new plastic from raw materials. In contrast, chemical recycling of polyesters can yield purified monomers that facilitate the production of virgin-like plastics. For instance, polyester can be converted to monomers via methanolysis catalyzed by transesterification catalysts such as zinc acetate, operating in either acidic or basic environments, although catalyst efficiency is currently limited.[28] Similarly, other organocatalysts, depending on their protonation state, can act as bases or acids due to their diverse chemical structures.[29–32] In polyester aminolysis, primary and secondary amines, with active hydrogen in their amino groups, can undergo nucleophilic substitution with polyester monomers to produce diamides.[33] Conversely, tertiary amines, characterized by a nitrogen atom linked to three alkyl or aryl substituents, serve as stable base catalysts that enhance transesterification while suppressing aminolysis.[34] Adjusting the Lewis basicity of tertiary amines is possible through functional group modification and steric hindrance. Tertiary amines, being volatile and easily separable, offer a more promising avenue for depolymerizing polyesters into monomers due to their distinct structures and properties when compared to traditional metal catalysts.[35,36]

In this study, we employed a variety of tertiary amine catalysts, which were distinguished by unique structures and basicity, to facilitate PET depolymerization through methanolysis. Notably, our results underscore the exceptional efficacy of N-methylpiperidine (NMP) as a catalyst, driving PET depolymerization with remarkable efficacy. Moreover, our inquiry extended to other polyesters, encompassing polylactic acid (PLA), polycarbonate (PC), and PBT, yielding impressive monomer or derivative yields. Particularly significant is our successful recycling of post-consumer PET derived from textiles, mixed plastic waste, and multilayer packaging materials, yielding substantial monomer yields (>90%). To deepen our understanding, we meticulously unraveled the PET depolymerization reaction mechanism using *in situ* magic-angle spinning (MAS) nuclear magnetic resonance (NMR) characterizations coupled with *ab initio* molecular dynamics (AIMD) calculations.

RESULTS AND DISCUSSION

Catalytic performance

PET decomposition reactions were conducted in a methanol solution at 160°C under 1 bar of nitrogen atmosphere. The catalytic performances of four types of tertiary amines were evaluated, including (1) linear amines: triethylamine and tripropylamine; (2) cyclic amines: NMP and 1,8-diazabicyclo[5.4.0]undec-7-ene (DBU); (3) aromatic amines: N,N-dimethylaniline and 4,N,N-trimethylaniline; and (4) diamines: N,N,N′,N′-tetramethyl-1,3-propanediamine, N,N,N′,N′-tetramethylethylenediamine, and N,N,N′,N′-tetraethylethylenediamine (Figure 1A). The main products of PET methanolysis are dimethyl terephthalate (DMT) and ethylene glycol (EG) (Figure 1B). Here, tertiary amines also act as co-solvents. The decomposition performances with and without tertiary amine catalysts for methanolysis of PET are listed

Cell Press
OPEN ACCESS

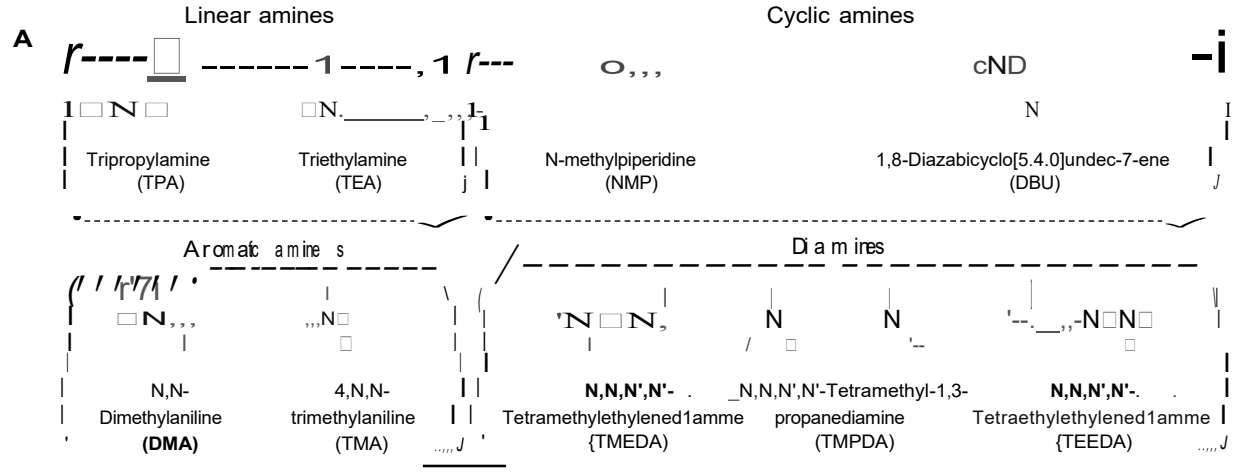

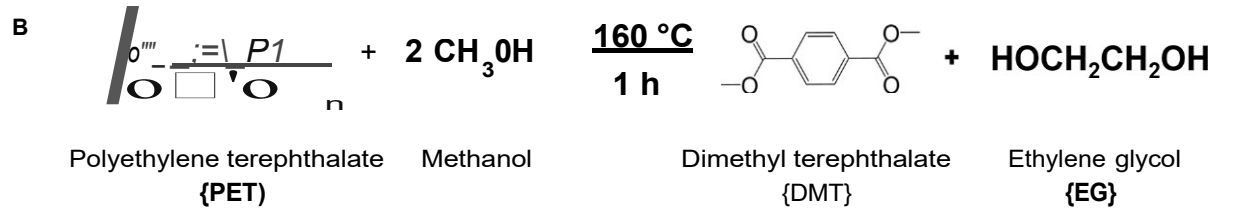

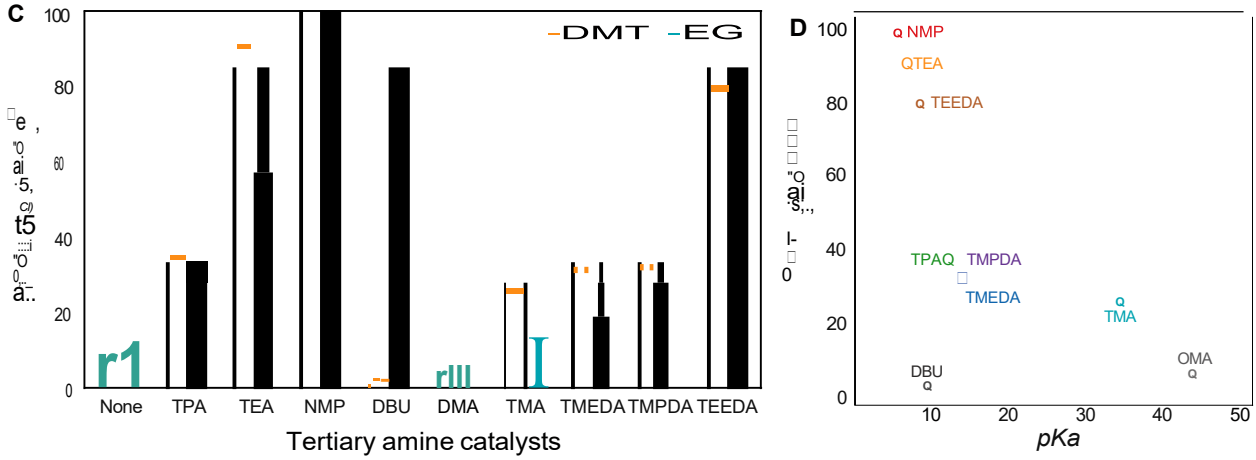

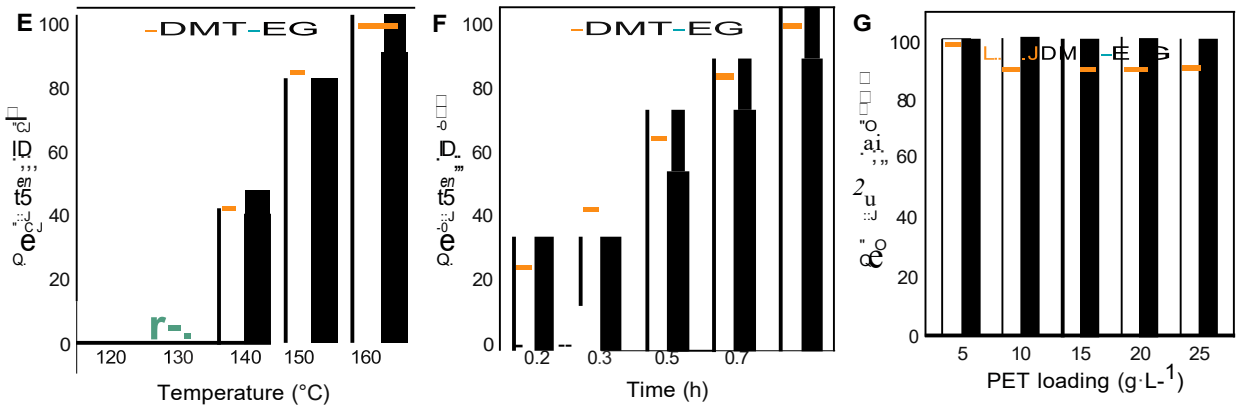

Figure 1. Catalytic performance for decomposition of PET with tertiary amines

(A) The chemical structural formulas of various tertiary amines.

(B) Reaction scheme of PET methanolysis reaction.

(C) Screening of tertiary amine catalyst for PET methanolysis reaction. Reaction conditions: 0.1 g of PET, 20 mL of 0.20 M tertiary amine in methanol solution, 160°C, 1 h, 700 rpm.

(D) Correlation between the pKa of the tertiary amine catalyst and the yield of DMT for methanolysis of PET.

(E–G) The effects of (E) temperature, (F) reaction time, and (G) PET loading amount on the DMT and EG yields of PET methanolysis with the NMP catalyst.

in Figure 1C and Table S1. Firstly, it is demonstrated that 13.1% of DMT and 12.0% of EG yields were obtained in the absence of any catalyst at 160°C for 1 h (yield calculation, please see the supplemental information). Notably, among all the tertiary amine catalysts tested, 100% of DMT and EG yields were obtained over the NMP catalyst. The DMT and EG yields are comparable to those with zinc(II) acetate catalyst and microwave heating at the same reaction temperature.[36] Various tertiary amines show a significant difference in yield of products. In order to elucidate the correlation between properties of tertiary amines and performance of PET methanolysis, the basicity of tertiary amine was quantified by pKa value (Table S2), which was calculated by the AIMD method. In terms of DMT yield, the efficiency of a tertiary amine catalyst in depolymerizing PET was correlated well to its basicity, except for the DBU catalyst, as shown in Figure 1D. When DBU was used as catalyst, the yield of DMT was only 3.1%, whereas the yield of EG was up to 83.3%. The high yield of EG indicated that the activity of PET decomposition was also high, which was also in line with the trend between basicity (pKa) and performance. It is attributed to the decomposition of DBU as the temperature reaches 140°C. The exposed N atom in the DBU derivatives can react with terephthalate through amidation, leading to the low yield of DMT, and the possible byproducts are listed in Figure S1. A higher yield of DMT was obtained with a weaker basicity of tertiary amine catalyst. Hence, the structural thermal stability and basicity of tertiary determined the catalytic performance of PET depolymerization.

The effect of reaction conditions on the catalytic performance of NMP was also investigated (Figures 1E–1G). The yields of DMT and EG were highly dependent upon the reaction temperature. A negligible reaction occurred at 120°C. Increasing the temperature to 160°C, the yields of DMT and EG reached 100%. Besides, the DMT and EG yields proportionally increased while increasing the reaction time, and it only took 1 h to complete the PET depolymerization. When increasing the PET loading amount from 5 to 25 g/L, the yields of DMT and EG still keep at 100%. The NMP catalyst was subjected to successive reaction cycles at 160°C for 30 min to evaluate its stability. It was found that both DMT and EG yields were maintained at ~50% during five reaction cycles (Figure S2). The NMP-catalyzed PET methanolysis process exhibited efficiency and stability, supporting its potential for scalability.

Due to the high efficiency of NMP for the catalytic deconstruction of PET, in the subsequent experiments, we extended this chemical recycling strategy to deconstruct other polyesters, including PLA, PC, and PBT. The catalytic performances of various polyesters using an NMP catalyst in the methanol solution are shown in Figure 2. Herein, the PLAs 4043D, 6060D, 6202D, and 2500HP were deconstructed into methyl lactate with >90% yields at 100°C, which are significantly higher than that in the absence of the NMP catalyst (Figures 2A and S3). For the decomposition of PC, a nearly 100% yield of bisphenol A was obtained at 120°C, much lower than a catalyst-free system (Figures 2B and S4). In terms of PBT (Figure 2C), the structure of PBT is similar but more resilient to alkali treatment than PET. It can achieve 100% of the DMT yield and 95.0% of the 1,4-butanediol yield at 160°C in an NMP-methanol system for PBT decomposition. The results indicated that all the

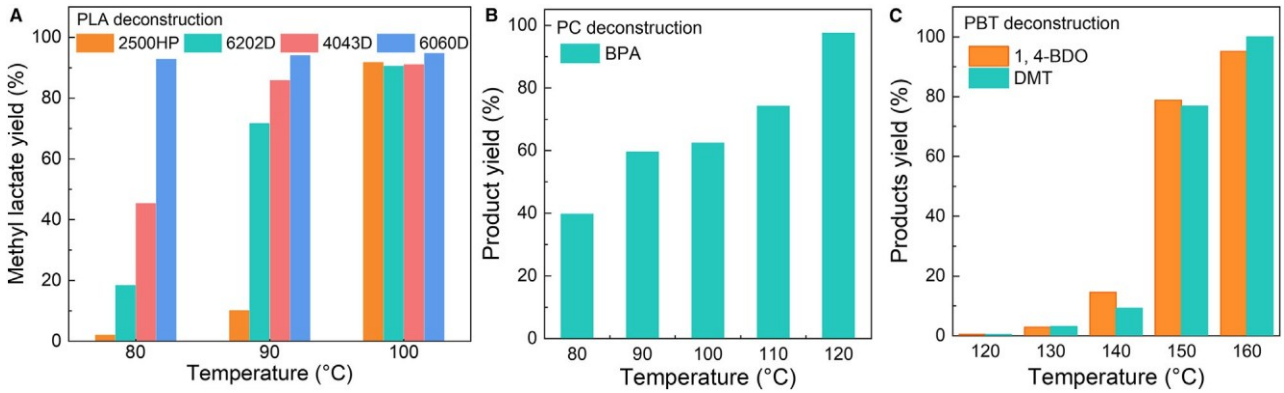

Figure 2. Decomposition of different polyesters with NMP catalyst under different temperatures in methanol solution

(A) Polylactic acid.

(B) Polycarbonate.

(C) Polybutylene terephthalate.

Reaction conditions: 0.1 g of polyester feedstock, 20 mL of 0.20 M NMP in methanol solution, 1 h, 700 rpm.

above polyesters could be efficiently deconstructed into monomers under a lower temperature in the presence of the NMP catalyst.

The chemical recycling/upcycling methods presented in the literature often assume that a single source of PET is readily accessible.[37] However, most post-consumer waste PET is mixed with other polymers and has other contamination, such as dyes. The cost is still high to sort PET from plastic waste. For example, the separation of PLA and PET is challenging due to their similar density and property. The PLA can contaminate the PET waste stream, resulting in poor recovery and a high cost of separation. The depolymerization temperatures for PET and PLA are different. We developed a sequential catalytic process for PLA and PET decomposition to depolymerize them using the NMP catalyst under different temperatures. The yields to methyl lactate, DMT, and EG were about 100%, as shown in Figure 3A. Additionally, selectively recycling PET in the waste plastic mixture containing various polymer components such as polyolefins and polyamide is challenging. To demonstrate the selective deconstruction of PET in plastic mixtures using the NMP catalyst, PET mixed with PE, polypropylene (PP), polystyrene (PS), and nylon 6 was used as feedstocks to deconstruct the methanol solution at 160°C for 1 h. As shown in Figure 3B, the yields of DMT and EG remained above 95%, indicating that other polymers show a slight effect on the PET depolymerization reaction. In addition, commercial multilayer packaging materials also contain PET and other plastic films, which are only disposed of by landfill and incineration and are difficult to recycle. To demonstrate the efficiency of PET deconstruction from packaging materials, commercial milk bags (PET/PA/PE, PA is polyamide) and vacuum seal storage bags (PET/PE) were added as feedstocks using the NMP catalyst in a methanol solution. The quantitative analysis of the PET composition in multilayer samples was determined by ^{1}H NMR analysis using the calibration curve method.[38] As can be seen in Figure 3C, about 90% of DMT and EG yields were obtained in the above system. The solid residues isolated from the reactor were essentially close to pure low density PE or PA, as demonstrated by the ^{1}H NMR spectra (Figure S5) and the XRD patterns (Figure S6). The findings suggested that it is feasible to recycle PET from packaging material.

It cannot be ignored that PET fibers are widely used in the textile industry.[39] However, PET is often mixed with other fabric materials and dyes in the textile industry. The

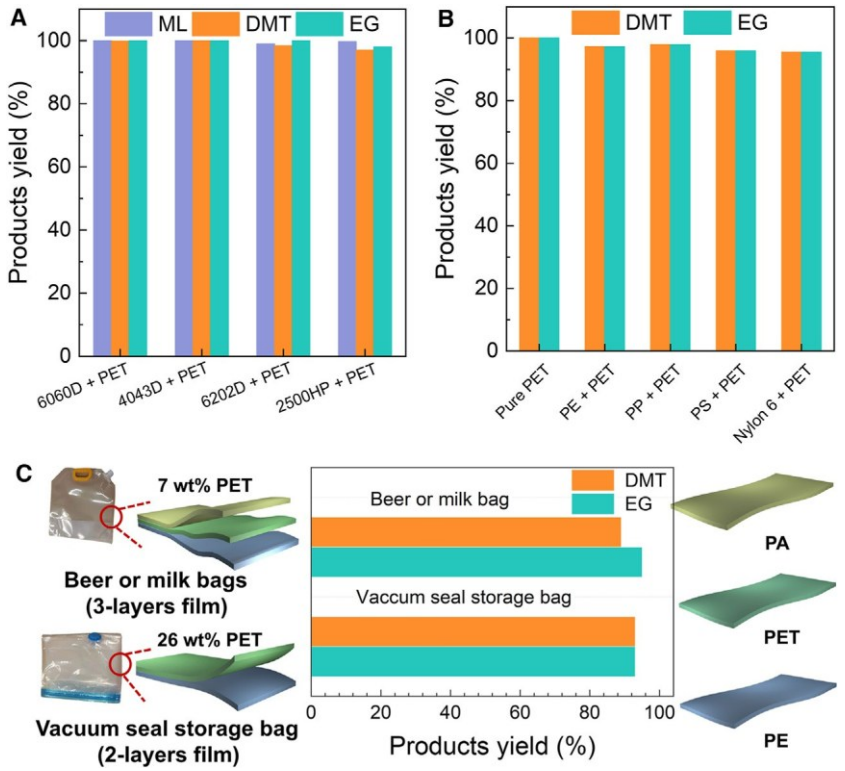

Figure 3. Selective deconstruction of PET from plastic mixtures and multilayer plastic packaging materials

(A) Deconstruction of PLA and PET mixture via the sequential process. Reaction condition: 0.5 g of PLA and 0.5 g of PET in 20 mL of 0.4 M NMP methanol solution, 700 rpm. Step 1: PLA 6202D: 90°C, 2 h; PLA 4043D: 80°C, 2 h; PLA 6060D: 60°C, 2 h; or PLA 2500HP: 90°C, 2 h. Step 2: PET: 160°C, 1 h, 700 rpm.

(B) Deconstruction of PET in PET/PE, PET/PP, PET/PS, or PET/nylon 6 mixture. Reaction condition: 0.1 g of PET and 0.1 g of other polymer, 20 mL of 0.2 M NMP methanol solution, 160°C, 1 h, 700 rpm.

(C) Deconstruction of post-consumer multilayer packaging materials, which contained PET/PA/PE or PET/PE. Reaction condition: 0.25 g multilayer film, 20 mL of 0.2 M NMP methanol solution, 160°C, 1 h, 700 rpm.

presence of dyes on textiles especially brings additional challenges to recycling post-consumer PET textiles since dyes could be detrimental to the environment. In the NMP-catalyzed deconstruction process, high yields of EG (90.8%) and DMT (89.5%) were obtained from the degradation of post-consumer PET textile with organic pigments sample at 160°C, as shown in Figure S7. A complete conversion of the post-consumer PET textile was accomplished within 30 min. Most of the organic pigments have -NHR, -NR_2, -NHCOR, -COR, and -OR groups (Figure S8),[40] which could compete with NMP in the methanolysis of PET and result in the production of byproducts. Since dispersed dyes are soluble in organic solvents such as methanol, methanol extraction pretreatment was carried out to remove dyes from textiles. The yield of DMT and EG evidently improved to 97.2% and 96.2% (Figure S9) after methanol extraction pretreatment. For comparison, the DMT and EG yields only changed slightly after the decolorization pretreatment with acetone or the mixture of acetone and methanol. Hence, methanol extraction pretreatment is necessary for colored waste PET to remove dyes with amine groups, which could improve the decomposition performance of PET.

NMR characterizations

Even though we have addressed concerns regarding structure stability and the basicity of tertiary amines, an in-depth investigation of the reaction mechanism is still essential to gain a comprehensive understanding of the processes involved and optimize the PET depolymerization performance. *In situ* MAS NMR was performed to explore the reaction pathway and molecular interaction under reaction conditions.[41,42] Figure 4A shows *in situ* ^{1}H MAS NMR spectra of PET decomposition on a sample containing PET, NMP, and methanol. Initially, the signal is relatively broad at 25°C due to the reduced mobility of the NMP catalyst and methanol, which are absorbed on the PET surface. The ^{1}H MAS NMR spectra of solid PET at ambient temperature are observed to be too broad due to strong homonuclear dipolar interactions among rigid protons in solid-state PET and the limited sample spinning rate of 4 kHz. Increasing the temperature to 140°C and maintaining it for 30 h, it is obvious that all the signals become sharper due to significantly increased molecular motion accompanied by the depolymerization of PET to monomer products. The yellow marked signals of ^{1}H NMR resonances assigned to the hydrogen associated with PET gradually decrease and ultimately disappear with reaction time, indicating the complete decomposition of PET. Meanwhile, the signals labeled with ''red'' and ''purple'' colors, which were attributed to target products, i.e., DMT and EG, respectively, slowly increased with time. The proton signals corresponding to the hydroxyl group of methanol and EG overlapped and gradually shifted downfield (i.e., chemical shifts increased) with time, highlighted by a red dashed arrow. Such a continuous downfield shifting is strong and direct evidence that protons of methanol are constantly transferred to form EG to break the ester bond of PET. Moreover, the EG signal became larger as the reaction time was extended, which further demonstrated this transesterification reaction.

To clearly monitor the reaction process and molecular interaction, *in situ* ^{13}C MAS NMR with well-resolved ^{13}C signals was employed, as shown in Figure 4B. The amplitude of PET (yellow marked) decreased while the intensities of DMT (red marked) and EG (purple marked) increased along with the reaction. It is also found that the yellow marked signal (PET) shifted from low to high chemical shifts, i.e., signals at 46.4 and 56.6 ppm shifting to 63.5 ppm and signals at 23.9 and 25.9 ppm shifting to 20.7 ppm, suggesting that there are molecular interactions between NMP, PET, methanol, and the reaction products (i.e., EG and DMT). Owing to an excessive amount of NMP, the signals of the initial NMP solution are still present at low intensity after the reaction. To clarify the strong interaction, we introduced only 5 mL of NMP to the reaction solution. As shown in Figure S10, the original NMP signals simply change and migrate downfield due to the complete onset interaction between all the NMP molecules and the environments (i.e., PET, reaction products, and methanol), in line with signals shifting in Figure S11.

To explore the origin of molecular interaction, *in situ* ^{1}H MAS NMR spectra on various samples with the following combinations were carried out: NMP and methanol; NMP, EG, and methanol; NMP, EG, methanol, and DMT; NMP and DMT; and NMP and PET (Figures 5A and 5B). Computational modeling (density functional theory [DFT]-NMR) of the ^{1}H chemical shifts was also carried out to explain the observed chemical shift trends and establish a physical picture of the interaction mechanisms, and the results are summarized in Figure 5C. The signal of the hydroxyl (-OH) proton associated with methanol demonstrated a downfield shift (5.09 ppm) in the sample of NMP and methanol compared to that of pure methanol (4.83 ppm), implying the formation of hydrogen bond between NMP and methanol, as shown in Figure 5A. The downfield shift is confirmed by NMR chemical shift computational modeling

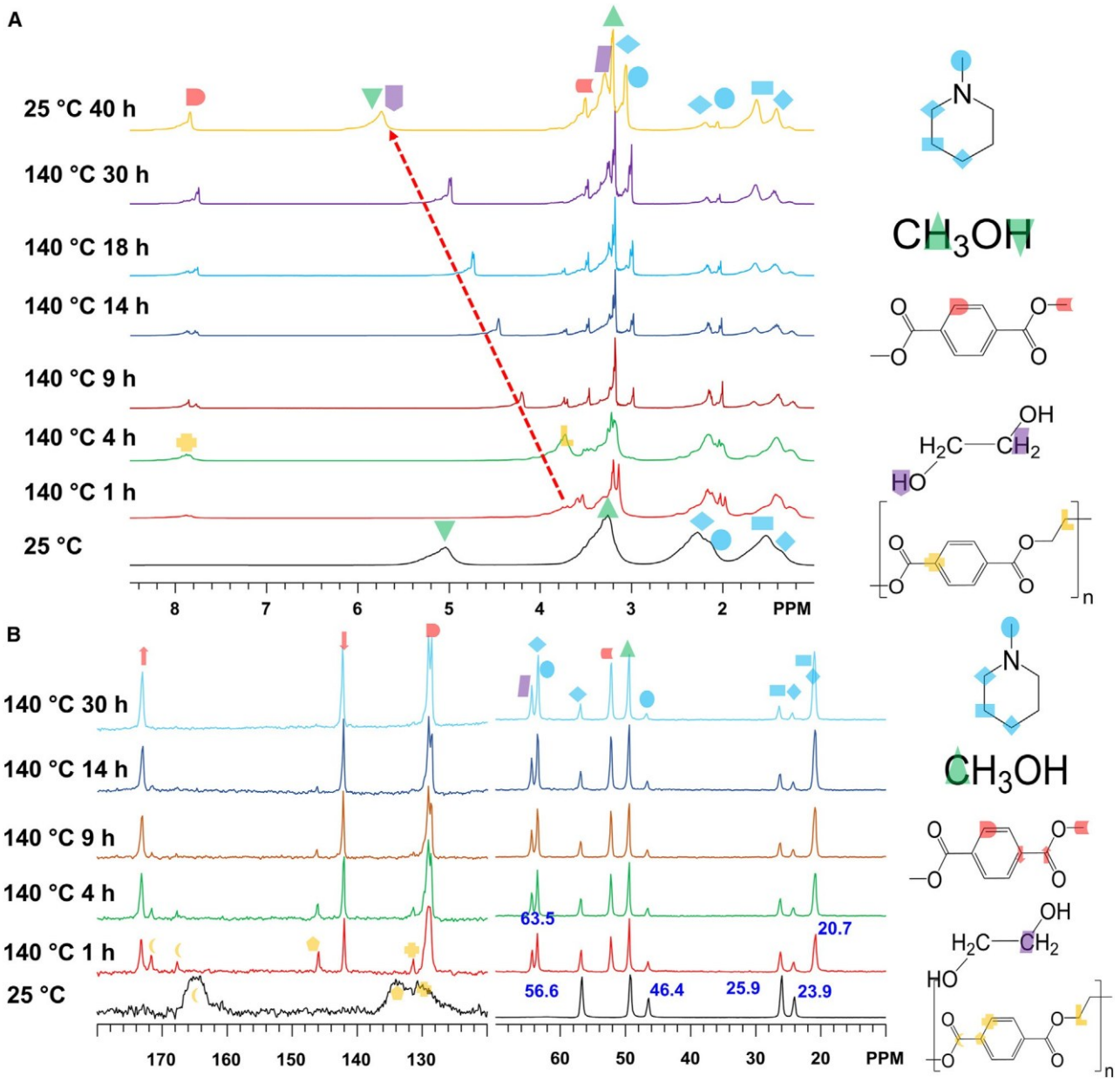

Figure 4. *In situ* NMR characterization

(A) *In situ* ^{1}H MAS NMR spectra of 60 mg of PET depolymerization with 100 mL methanol and 100 mL of NMP at different temperatures with time on stream (from bottom to top). Pulse width: 2.5 ms, acquisition time: 650 ms, recycle delay: 4 s, reaction time: 40 h.

(B) *In situ* ^{13}C MAS NMR spectra of 60 mg of PET depolymerization with 100 mL of methanol and 100 mL of NMP at different temperatures with time on stream (from bottom to top). Pulse width: 2.5 ms, acquisition time: 205 ms, recycle delay: 10 s, reaction time: 40 h.

on models (2) and (3) in Figure 5C, where a single methanol molecule (Figure 5C2: gas phase) and a pair of NMP-methanol (Figure 5C3: the proton of hydroxyl from methanol is hydrogen bonded to N of NMP) are used to show the trend of the shift. The hydrogen bond elongates the O–H bond distance from 0.97 to 1.01 A$^{\circ}$, promoting the nucleophilicity of oxygen in methanol.

As mentioned in Figures 4A and S11, the four signals of NMP all shift drastically downfield during the reaction; however, the NMP-methanol and NMP, EG, and

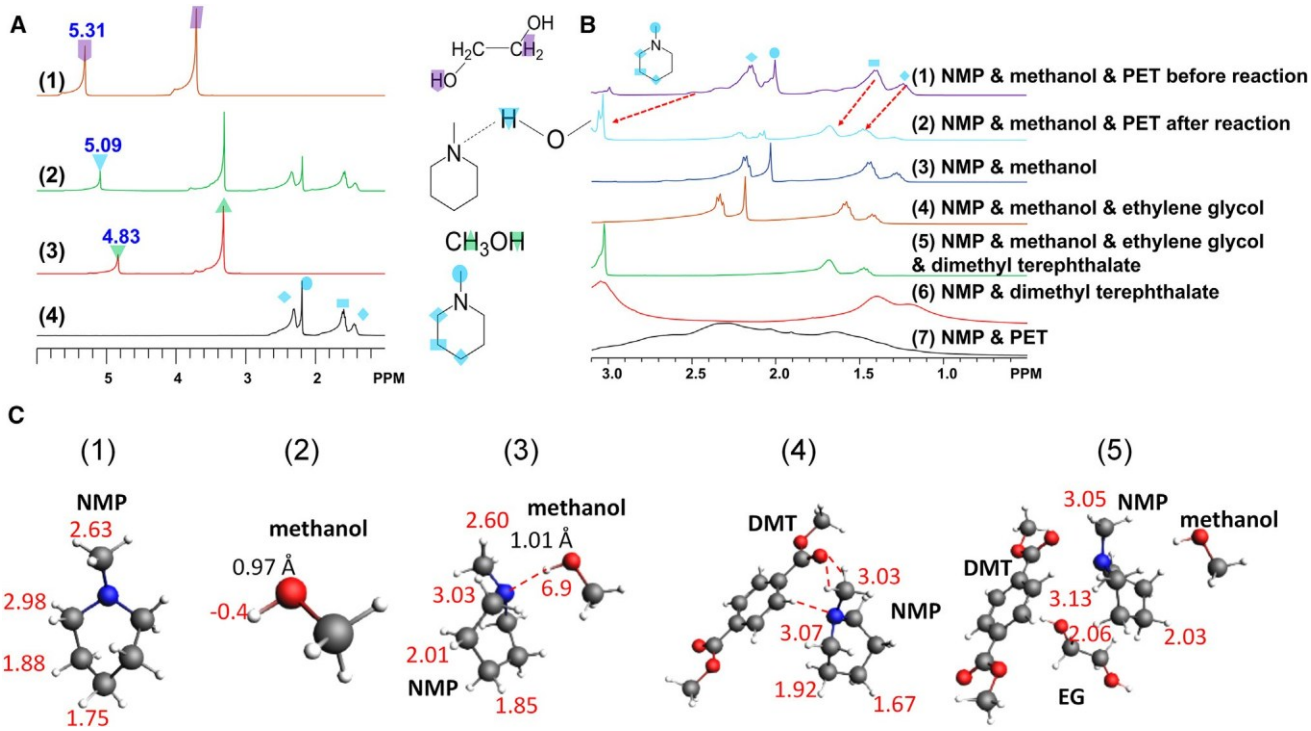

Figure 5. *Ex situ* NMR characterization

(A) Comparison of *in situ* ^{1}H MAS NMR spectra of (1) EG, (2) NMP and methanol 1:3 M ratio, (3) methanol, and (4) NMP at 25°C.

(B) Different combinations in terms of signals ranging from 3.1 to 0.5 ppm. (1 and 2) *In situ* NMR of reaction; (3) NMP and methanol; (4) NMP, EG, and methanol; (5) NMP, EG, methanol, and DMT; (6) NMP and DMT; and (7) NMP and PET. Temperature: 140°C.

(C) DFT-NMR modeling of (1) NMP, (2) methanol, (3) NMP with methanol, (4) NMP with DMT, and (5) NMP with methanol, EG, and DMT. Geometries were optimized by using the GGA applied to Becke-Lee-Yang-Parr (BLYP) functional. TZ2P is used as a basis set. The numbers represent the chemical shifts of each signal and bond distance. The symbols with different colors and shapes represent different positions of hydrogen atoms and carbon atoms in different chemicals.

methanol mixtures hardly show such significant shifts (Figure 5B). It was observed that the signals shift dramatically in the NMP, EG, methanol, and DMT mixture, indicating a crucial interaction between NMP and DMT. It can be deduced that methyl and methylene groups form hydrogen bonds with the carbonyl oxygen of DMT, resulting in significant chemical shifts. DFT-NMR computational modeling on cluster models in Figure 5C4 justifies the above hypothesis, where the chemical shifts of methyl and methylene groups, indeed, changed due to two kinds of hydrogen bonds, i.e., with one between N of NMP and H of the benzene ring of DMT and another one between the carbonyl oxygen of DMT and methyl H of NMP, as shown with red dashed line in model 4. This hydrogen bond or interaction with carbonyl oxygen is consistent with previously proposed evidence.[43] Nonetheless, there is no chemical shift associated with three methylene groups away from the N atom when NMP interacts exclusively with DMT, implying that only the CH_3 and CH_2 close to N strongly interact with DMT, while methylene groups further away from the N atom have no interaction with DMT. Thus, the three methylene groups shifting downfield during the operando reaction can be correlated with the hydrogen bonding network with EG and methanol, demonstrated in calculation model (4) (Figure 5C4), which shows downfield shifting with those three methylene hydrogens. It is worth noting that when NMP only interacts with PET, there are no such signal shifts, which is most likely due to the steric inhibition effect of the rigid structure of PET and the low surface area of the PET particles. Regarding methanol's interaction with

other chemicals (Figure S12), the most evident shift is displayed with the proton of the methanol -OH group, which shifts from 3.92 to 4.77 in the presence of DMT. This dramatic shift clearly shows that methanol can donate electrons to electrophilic DMT to affect the DMT structure.

Combining the findings mentioned earlier and considering that DMT is a monomer of PET, the NMP/PET/methanol interaction mechanism may be similar to when DMT interacts with NMP and methanol, i.e., NMP forms hydrogen bonds with methanol and also with PET carbonyl oxygen. After the carbonyl oxygen of PET is activated by hydrogen bonding, the oxygen of methanol with enhanced nucleophilicity by hydrogen bonding with NMP can readily attack the carbonyl carbon of PET to break the ester bond. The methanol hydrogen is then transferred to EG, and the produced EG also joins the hydrogen-bonding network.

Ex situ NMR characterization was also conducted to probe the PET depolymerization mechanism. The ^{1}H NMR spectra of the fresh and residual PET samples are almost identical, indicating that no oligomers or byproducts were formed and deposited on the residual PET samples, as shown in Figure S13. The ^{1}H NMR spectra of the products after partial depolymerization of PET demonstrated that DMT and EG are the dominant liquid-phase products after a reaction of 0.2 h, as shown in Figure S14. Likewise, no oligomer signals were observed in the liquid-phase product samples. This result is confirmed by comparing the ^{1}H NMR spectra of the pure DMT and EG (Figure S15). Hence, it can be considered that PET undergoes chain-end scission during the NMP-catalyzed methanolysis rather than random scission in supercritical methanol.

Proposed reaction pathway

Based on the above *in situ* NMR analysis, a possible reaction pathway for NMP-catalyzed methanolysis of PET is shown in Figure 6. (1) Firstly, NMP dissolves in a methanol solution. The free electrons of N in the NMP structure enable it to act as a Lewis base. This allows NMP to extract a proton from methanol, forming the methanol/NMP complex that enhances the nucleophilicity of the oxygen in methanol. (2) Additionally, two types of hydrogen bonds contribute to the activation of ester bonds. One type involves the nitrogen atom of NMP and the hydrogen atom of the benzene ring of PET, while the other involves the carbonyl oxygen of PET and the methyl hydrogen atom of NMP. (3) The activated oxygen in methanol attacks the activated carbonyl group in a PET polymer unit, causing an electron transfer of the ester bonds.[44] (4) This rearrangement of electrons leads to the formation of hydrogen bonding with the backbone oxygen of PET and methoxide transfer, creating a tetrahedral intermediate. (5) The formation of a new alcohol and restoration of the amine catalyst results in the formation of DMT and EG monomers and the corresponding chain-cut PET. The chain-cut PET is further catalyzed to generate the final products, DMT and EG, by the same mechanism. Catalyzed by the transesterification reaction, PET repeating units are isolated from the PET polymer via chain-end scission. As a result, the final depolymerization products, DMT and EG, are obtained. This mechanism is different from the traditional random scission mechanism in the methanolysis of PET under supercritical conditions.[45]

In summary, we have developed a simple and efficient chemical sorting strategy that selectively deconstructs post-consumer PET into DMT and EG with ~100% yields using the NMP catalyst in a methanol solution. The catalytic performance of distinct tertiary amine catalysts correlated with their structures and basicity. Furthermore, this approach has demonstrated successful depolymerization of other polyesters like

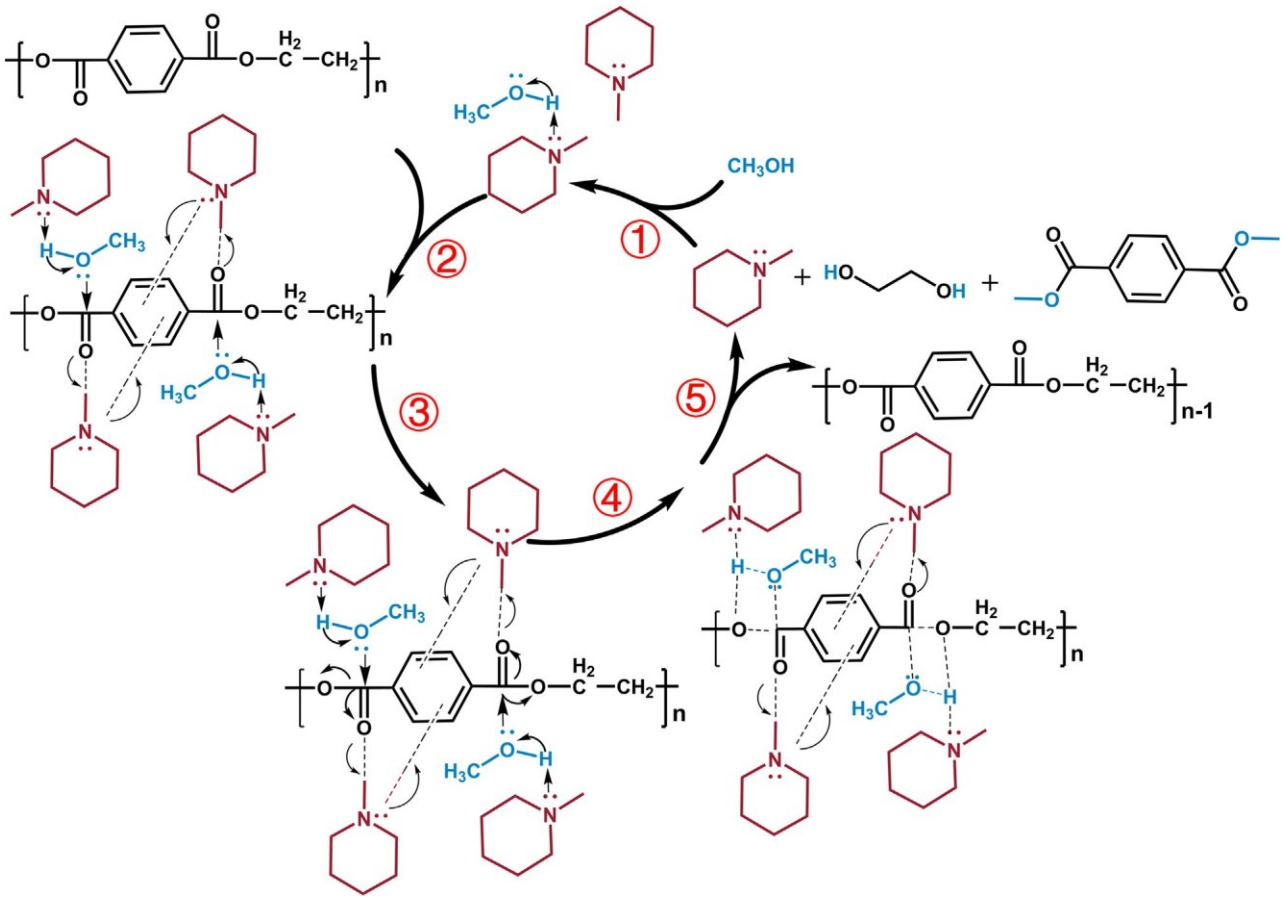

Figure 6. Reaction mechanism for decomposition of PET with NMP catalyst in methanol solution

(1) Formation of methanol/NMP complex, (2) formation of hydrogen bonds, (3) reaction of ester bond, (4) formation of tetrahedral intermediate, and (5) desorption of DMT, EG, and chain-cut PET.

PLA, PBT, and PC, yielding their respective monomers. Notably, even in the case of PET present in plastic mixtures, multilayer packaging materials, and textiles, substantial DMT and EG yields were achieved. This method holds promise as a molecular-level solution for sorting PET from post-consumer plastic waste. AIMD calculations corroborate the assumption made based on the NMR results, leading to the suggested mechanism that NMP acts as a Lewis base catalyst, extracting a proton from methanol, thereby enhancing methanol's nucleophilicity. Two types of hydrogen bonds, i.e., one between NMP's N atom and PET's benzene ring's H atom and the other between PET's carbonyl O atom and NMP's methyl H atom, contribute to PET's ester bond activation. The nucleophilic attack of methanol's oxygen atom on PET's carbonyl carbon atom leads to the cleavage of PET's C–O bond and the formation of DMT's C–O bond. This work presents a catalytic chemical sorting method for depolymerizing waste plastic polyesters into monomers, offering fresh perspectives on a promising alternative for closed-loop recycling of polyester waste.

EXPERIMENTAL PROCEDURES

Resource availability

Lead contact

Further information and requests for resources should be directed to and will be fulfilled by the lead contact, Hongfei Lin (hongfei.lin@wsu.edu).

Materials availability

This study did not generate new materials.

Data and code availability

Data relating to the materials, methods, experiment procedures, and other characterizations are available in the supplemental information. All other data are available from the authors upon reasonable request.

Materials

The post-consumer PET sample was a Kirkland Signature Premium Drinking Water bottle. The PET textile sample was provided by the Department of Apparel, Merchandising, Design, and Textiles at Washington State University. The commercial-grade PLA samples 4043D, 6060D, 6202D, and 2500HP were donated by NatureWorks. The PC sample was a Corning square polycarbonate storage bottle from Sigma-Aldrich. The PBT sample was purchased from Sigma-Aldrich. Other plastics, including PE, PP, PS, and nylon 6, were purchased from Sigma-Aldrich. The multilayer packaging materials, including PET/PA/PE film for beer/milk packages and PET/PE film for vacuum seal storage, were purchased from Walmart.com. Quantitative analysis of PET in multilayer samples was carried out by ^{1}H NMR spectroscopy using the calibration curve method.[38] Methanol (EMD Millipore, R99.8%), NMP (Sigma-Aldrich, 99%), tripropylamine (Sigma-Aldrich, R98%), triethylamine (Alfa Aesar, 99%), N,N-dimethylaniline (Sigma-Aldrich, 99%), 4,N,N-trimethylaniline (Sigma-Aldrich, 99%), DBU (Sigma-Aldrich, 98%), N,N,N^{0},N^{0}-tetramethylethylenediamine (Alfa Aesar, 99%), N,N,N^{0},N^{0}-tetramethyl-1,3-propanediamine (Sigma-Aldrich, 99%), N,N,N^{0},N^{0}-tetraethylethylenediamine (Sigma-Aldrich, 98%), 1,1,1,3,3,3-hexafluoro-2-propanol (HFIP; Alfa Aesar, 99%), chloroform-d (Sigma Aldrich, 99.8 atom %D, contains 0.03% [v/v] TMS), acetone (Avantor Performance Materials, 99.3%), DMT (Sigma-Aldrich, R99%), EG (Sigma-Aldrich, 99.8%), 1,4-butanediol (Sigma-Aldrich, 99%), methyl(S)-(−)-lactate (Alfa Aesar, 97%), and bisphenol A (Sigma-Aldrich, R99%) were used in our study. All chemicals were acquired in their pure form and utilized without any prior treatment.

Catalytic performance evaluation for polyesters depolymerization with tertiary amines

The catalytic reactions were performed in the Multiple Reactor System (Parr Series 500, 45 mL) incorporated with the temperature controller (4871 series). Generally, the reactants (PET bottle sample, PET textile sample, PLA pellets, PC bottle sample, PBT pellets, plastics mixture, or multilayer packaging films), the solvent (methanol), and a selected volume of tertiary organic amine catalyst were placed in the vessels. The vessels were sealed and purged three times with N_2. The reactor was full of N_2 under ambient pressure at room temperature. The reaction mixture was subjected to simultaneous magnetic stirring (700 rpm) and heating to the set temperature (30 min) and kept at the set temperature for the set reaction duration. After the reaction, the reaction vessels were immediately quenched in cooling water for fast cooling.

The PET methanolysis reactions with NMP were repeated five times during the catalyst stability test. After each run, the liquid in the vessel was collected and transferred into a centrifuge tube (50 mL) and subjected to centrifugation in an Eppendorf 5810 R Centrifuge. Then, the supernatant was filtered with a 0.45 mm polyethersulfone filter to remove the small PET particles. Next, a certain amount of 0.2 M NMP methanol solution was added until the apparent recycled solution volume reached 20 mL. Finally, the fresh PET sample (0.1 g) was added for the recyclability test.

The above recycling procedures were repeated five times to estimate the catalytic stability of NMP in the methanolysis of PET.

In order to separate the dyes and investigate the effect of dyes on the PET degradation performance, colored PET textiles were subjected to individual pretreatment with methanol, acetone, and a mixture of methanol and acetone. The pretreatment system was kept at 50°C while being stirred overnight. The PET textiles were then washed with the corresponding solvent at least three times and dried in air to obtain the white PET textiles. The methanolysis procedure of white PET textiles was the same as that of the colored PET textiles.

Product analysis method

Since there is no evidence of gas product formation, the reactor was disassembled without venting after a reaction. The vessels were rinsed with the solvent, and the solid residues were collected. All the liquid phases were subjected to filtration (0.45 mm syringe filter) prior to analysis. The liquid phase was then analyzed by a GCMS QP-2020 (Shimadzu) to investigate the unknown components, and both GCMS QP-2020 and GC-FID (GC-2010, Shimadzu) were used to quantify the products. After the determination of the product contents, the yields of the DMT (*D*) and the EG (*E*) were calculated by the following equations.

$$D = \frac{n_1}{n_0} \times 100\ \%\ \text{and} \qquad \text{(Equation 1)}$$

$$E = \frac{n_2}{n_0} \times 100\ \%; \qquad \text{(Equation 2)}$$

where n_0 is the moles of the repeat unit of fresh PET reactants before the reaction, n_1 is the moles of DMT after the reaction, and n_2 is the moles of EG after the reaction. The yields of other monomers or esters from other polyesters were also calculated following a similar procedure.

In situ ^{1}H and ^{13}C MAS NMR measurements

Operando (*in situ*) ^{1}H and ^{13}C MAS NMR measurements were carried out using a Varian-Agilent Inova wide-bore 300 MHz NMR spectrometer employing a commercial 7.5 mm Vespel pencil type MAS probe, functioning at ^{1}H and ^{13}C Larmor frequencies of 299.969 and 75.42 MHz, respectively. A sample spinning rate of about 4 kHz was used to produce a high-resolution ^{1}H and ^{13}C MAS NMR spectrum on a heterogeneous system containing a mixture of PET, catalysts, and solvents. A special *in situ* MAS NMR rotor[41] capable of perfectly sealing a mixture containing solid, liquid, and gaseous phases at elevated temperature and pressure was used. The volume of the sample cell space is 300 mL. A single pulse sequence was used for acquiring the ^{1}H signal, consisting of a pulse with a pulse width of 2.5 ms (equivalent to a pulse angle of 50°), an acquisition time of 650 ms, and a recycle delay of 4 s. For the ^{13}C MAS NMR signal, a pulse width of 2.5 ms (equivalent to a pulse angle of 45°), an acquisition time of 205 ms, and a recycle delay of 10 s were applied. All spectra were externally referenced to tetramethylsilane (TMS) (0 ppm) using adamantane as a second reference at 1.82 ppm for ^{1}H and 38.48 ppm for ^{13}C. The sample temperature was calibrated using EG as previously reported.[46]

Ex situ ^{1}H NMR measurement

^{1}H NMR measurement was conducted with a 400 Liquid State NMR (One Probe, X-tunable and ^{1}H) over 256 scans, a 1 s relaxation delay, and a 45° pulse angle. The fresh and residual samples, liquid product, standard DMT sample, standard EG sample, HFIP, and NMP were tested by ^{1}H NMR.

For the NMR measurement of fresh PET, one piece of scrap from a transparent PET bottle was dissolved in 1 mL of HFIP, and then 1 mL of chloroform-d (99.8 atom %D, contains 0.03% [v/v] TMS) was added when PET was completely dissolved. For the NMR measurement of residues after a reaction, the residual was separated from the liquid products by centrifugation in an Eppendorf 5810 R Centrifuge. The residual samples or the liquid products were dried in a fume hood overnight. The dried residual samples or liquid products were also dissolved in 1 mL of HFIP in a 2 mL autosampler glass vial, in which 1 mL of chloroform-d (99.8 atom %D, contains 0.03% [v/v] TMS) was also added. After the liquid was completely mixed, the supernatant was transferred into an NMR tube.

A fixed amount of NMP was dissolved in 1 mL of chloroform-d (99.8 atom %D, contains 0.03% [v/v] TMS), and the solution was transferred into an NMR tube. One piece of standard DMT sample and one drop of standard EG sample were dissolved in 1 mL of chloroform-d (99.8 atom %D, which contains 0.03% [v/v] TMS) separately, and the clear solution was also individually transferred into an NMR tube.

Quantum chemistry measurements

Computational modeling of the NMR chemical shifts was performed by employing the Amsterdam Density Functional (ADF-2017) package. Geometries were optimized by using the generalized gradient approximation (GGA) applied to the Becke-Lee-Yang-Parr functional.[47,48] Calculations were performed by using the all-electron TZ2P basis set (Triple-z, 2-polarization function) with Slater-type [49] orbitals implemented in the ADF program. NMR chemical shielding calculations were carried out based on the optimized geometrical structures at the same theory level and with the same basis set for each atom. The geometry-optimized structures at the same level of theory were applied to calculate the chemical shielding for each atom with the same basis set. Tetramethylsilane was used as the ^{1}H chemical shift reference by converting the calculated shielding to the observed shielding using the following equation: $d_{iso} = s(TMS) - s_{calc} = 31.4 - s_{calc}$. Based on previous publications,[50,51] cluster calculation will provide different absolute chemical shifts compared to the polarized continuum model, but they will not affect the trend of chemical shift changes. For simplicity, a cluster calculation is conducted to demonstrate the interaction between different molecules to simulate the trend of chemical shifting in experiments. Calculated models of DMT, methanol, NMP, and EG together in different conformations are provided in Figure S16. The one chosen in the main text is the most consistent with experimental trends.

AIMD pKa calculations

All calculations were carried out by using the Vienna Ab initio Simulation Package[52,53] within the projector augmented-wave approach.[54] The GGA Perdew-Burke-Ernzerhof exchange-correlation functional[55] was employed in combination with DFT-D3 Grimme to correct the long-range dispersion interactions.[56] The plane wave basis set cutoff energy was set to 400 eV.

The pKa calculations of catalysts considered in this study were done through protonation of the N atom of the catalyst by the H atom that terminates the PET monomer according to the following generalized Equation 3:

$$1\ \text{PET monomer} + 1\ \text{catalyst} + x\ \text{methanol} \rightleftharpoons 1\ \text{PET monomer}^{--} + 1\ \text{catalyst} \text{--} H^{+} + x\ \text{methanol}: \quad \text{(Equation 3)}$$

The reaction described in Equation 3 was split into a reactant and product, where each half of the reaction was simulated independently of the other half. For each half, a single molecule of either reactant or product together with one molecule of a particular catalyst was placed in a simulation cell of 10 3 10 3 10 $A^{\circ 3}$ subject to periodic boundary conditions. The simulation box was then filled with 3–5 methanol molecules, subject to the catalyst, to make up the density of approximately 0.8 g/cm^3. AIMD-based simulations were carried out at G-point with a time step of dt = 1 fs. Each system was initially equilibrated for at least 10 ps or until the simulation converged and was subsequently followed by 10 ps of production time. The Nose-Hoover thermostat was used to keep the simulation temperature at around 433 K, in accordance with experiment.[57,58]

The difference in averaged free energy between protonated and unprotonated was calculated, and the pKa was thus computed by using the following Equation 4:

$$pKa = \frac{DF}{2{:}303RT}; \quad \text{(Equation 4)}$$

where DF is the difference of the averaged free energy between the reactant half and the product half of the reaction, R is the gas constant, and T is the temperature at which the simulations were performed.

SUPPLEMENTAL INFORMATION

Supplemental information can be found online at https://doi.org/10.1016/j.xcrp.2024.102145.

ACKNOWLEDGMENTS

The funding was supported by NSF EFRI E3P award #2132219. The *in situ* MAS NMR experiments were supported by the US Department of Energy, Office of Science, Basic Energy Sciences, Chemical Sciences, Geosciences, and Biosciences Division, Catalysis Science program, FWP 47319.

AUTHOR CONTRIBUTIONS

H.L. and S.X. conceived the idea. H.L. supervised the project. S.X. and C.W. conducted most of the experiments and wrote and revised the manuscript. W.H., J.Z.H., and Y.W. performed the *in situ* MAS NMR experiment and analysis. N.N.I. and J.P. performed the AIMD calculations and analysis. Z.D. conducted some catalyst evaluation experiments. H.L., Y.W., J.P., and J.Z.H. managed the funds. All authors contributed to the discussion and revision of the manuscript.

DECLARATION OF INTERESTS

The authors declare a patent application. Lin, H. "Conversion of co-mingled waste plastics to monomers and fuels in sequential catalytic process." US patent application no. 18/251,958, filed November 9, 2021. Hosted at: https://ppubs.uspto.gov/dirsearch-public/print/downloadPdf/20240025085.

Received: March 24, 2024
Revised: June 24, 2024
Accepted: July 16, 2024
Published: August 6, 2024

REFERENCES

1. (2019). Plastic upcycling. Nat. Catal. *2*, 945–946. https://doi.org/10.1038/s41929-019-0391-7.
2. Geyer, R., Jambeck, J.R., and Law, K.L. (2017). Production, use, and fate of all plastics ever made. Sci. Adv. *3*, e1700782. https://doi.org/10.1126/sciadv.1700782.
3. Schyns, Z.O.G., and Shaver, M.P. (2021). Mechanical recycling of packaging plastics: a review. Macromol. Rapid Commun. *42*, e2000415. https://doi.org/10.1002/marc.202000415.
4. Coates, G.W., and Getzler, Y.D.Y.L. (2020). Chemical recycling to monomer for an ideal, circular polymer economy. Nat. Rev. Mater. *5*, 501–516. https://doi.org/10.1038/s41578-020-0190-4.
5. Tournier, V., Topham, C.M., Gilles, A., David, B., Folgoas, C., Moya-Leclair, E., Kamionka, E., Desrousseaux, M.L., Texier, H., Gavalda, S., et al. (2020). An engineered PET depolymerase to break down and recycle plastic bottles. Nature *580*, 216–219. https://doi.org/10.1038/s41586-020-2149-4.
6. Yoshida, S., Hiraga, K., Takehana, T., Taniguchi, I., Yamaji, H., Maeda, Y., Toyohara, K., Miyamoto, K., Kimura, Y., and Oda, K. (2016). A bacterium that degrades and assimilates poly(ethylene terephthalate). Science *351*, 1196–1199. https://doi.org/10.1126/science.aad6359.
7. Zhang, F., Zeng, M., Yappert, R.D., Sun, J., Lee, Y.H., LaPointe, A.M., Peters, B., Abu-Omar, M.M., and Scott, S.L. (2020). Polyethylene upcycling to long-chain alkylaromatics by tandem hydrogenolysis/aromatization. Science *370*, 437–441. https://doi.org/10.1126/science.abc5441.
8. Conk, R.J., Hanna, S., Shi, J.X., Yang, J., Ciccia, N.R., Qi, L., Bloomer, B.J., Heuvel, S., Wills, T., Su, J., et al. (2022). Catalytic deconstruction of waste polyethylene with ethylene to form propylene. Science *377*, 1561–1566. https://doi.org/10.1126/science.add1088.
9. Chen, S., Tennakoon, A., You, K.E., Paterson, A.L., Yappert, R., Alayoglu, S., Fang, L., Wu, X., Zhao, T.Y., Lapak, M.P., et al. (2023). Ultrasmall amorphous zirconia nanoparticles catalyse polyolefin hydrogenolysis. Nat. Catal. *6*, 161–173. https://doi.org/10.1038/s41929-023-00910-x.
10. Jia, C., Xie, S., Zhang, W., Intan, N.N., Sampath, J., Pfaendtner, J., and Lin, H. (2021). Deconstruction of high-density polyethylene into liquid hydrocarbon fuels and lubricants by hydrogenolysis over Ru catalyst. Chem Catal. *1*, 437–455.
11. Ugduler, S., Van Geem, K.M., Denolf, R., Roosen, M., Mys, N., Ragaert, K., and De Meester, S. (2020). Towards closed-loop recycling of multilayer and coloured PET plastic waste by alkaline hydrolysis. Green Chem. *22*, 5376–5394. https://doi.org/10.1039/d0gc00894j.
12. English, L.E., Jones, M.D., and Liptrot, D.J. (2022). N-heterocyclic phosphines as precatalysts for the highly selective degradation of poly(lactic acid). ChemCatChem *14*, e202101904. https://doi.org/10.1002/cctc.202101904.
13. Fang, P., Lu, X., Zhou, Q., Yan, D., Xin, J., Xu, J., Shi, C., Zhou, Y., and Xia, S. (2023). Controlled alcoholysis of PET to obtain oligomers for the preparation of PET-PLA copolymer. Chem. Eng. J. *451*, 138988. https://doi.org/10.1016/j.cej.2022.138988.
14. Wang, L., Nelson, G.A., Toland, J., and Holbrey, J.D. (2020). Glycolysis of PET using 1,3-dimethylimidazolium-2-carboxylate as an organocatalyst. ACS Sustain. Chem. Eng. *8*, 13362–13368. https://doi.org/10.1021/acssuschemeng.0c04108.
15. Fukushima, K., Coulembier, O., Lecuyer, J.M., Almegren, H.A., Alabdulrahman, A.M., Alsewailem, F.D., Mcneil, M.A., Dubois, P., Waymouth, R.M., Horn, H.W., et al. (2011). Organocatalytic depolymerization of poly (ethylene terephthalate). J. Polym. Sci. A. Polym. Chem. *49*, 1273–1281.
16. Fukushima, K., Coady, D.J., Jones, G.O., Almegren, H.A., Alabdulrahman, A.M., Alsewailem, F.D., Horn, H.W., Rice, J.E., and Hedrick, J.L. (2013). Unexpected efficiency of cyclic amidine catalysts in depolymerizing poly (ethylene terephthalate). J. Polym. Sci. A. Polym. Chem. *51*, 1606–1611.
17. Tian, S., Jiao, Y., Gao, Z., Xu, Y., Fu, L., Fu, H., Zhou, W., Hu, C., Liu, G., Wang, M., and Ma, D. (2021). Catalytic amination of polylactic acid to alanine. J. Am. Chem. Soc. *143*, 16358–16363. https://doi.org/10.1021/jacs.1c08159.
18. Teotia, M., Tarannum, N., and Soni, R.K. (2017). Depolymerization of PET waste to potentially applicable aromatic amides: Their characterization and DFT study. J. Appl. Polym. Sci. *134*, 45153. https://doi.org/10.1002/app.45153.
19. Song, K., Li, Y., Zhang, R., Wang, N., Liu, J., Hou, W., Zhou, Q., and Lu, X. (2023). Catalytic steam-assisted pyrolysis of PET for the upgrading of TPA. Materials *16*, 2362. https://doi.org/10.3390/ma16062362.
20. Jia, H., Ben, H., Luo, Y., and Wang, R. (2020). Catalytic fast pyrolysis of poly (ethylene terephthalate) (PET) with zeolite and nickel chloride. Polym. Bull. (Heidelberg, Ger.) *12*, 705. https://doi.org/10.3390/polym12030705.
21. Xie, S., Sun, Z., Liu, T., Zhang, J., Li, T., Ouyang, X., Qiu, X., Luo, S., Fan, W., and Lin, H. (2021). Beyond biodegradation: Chemical upcycling of poly(lactic acid) plastic waste to methyl lactate catalyzed by quaternary ammonium fluoride. J. Catal. *402*, 61–71. https://doi.org/10.1016/j.jcat.2021.08.032.
22. Wu, F., Wang, Y., Zhao, Y., Tang, M., Zeng, W., Wang, Y., Chang, X., Xiang, J., Han, B., and Liu, Z. (2023). Lactate anion catalyzes aminolysis of polyesters with anilines. Sci. Adv. *9*, eade7971. https://doi.org/10.1126/sciadv.ade7971.
23. Gao, Z., Ma, B., Chen, S., Tian, J., and Zhao, C. (2022). Converting waste PET plastics into automobile fuels and antifreeze components. Nat. Commun. *13*, 3343. https://doi.org/10.1038/s41467-022-31078-w.
24. Sun, B., Zhang, J., Wang, M., Yu, S., Xu, Y., Tian, S., Gao, Z., Xiao, D., Liu, G., Zhou, W., et al. (2023). Valorization of waste biodegradable polyester for methyl methacrylate production. Nat. Sustain. *6*, 712–719. https://doi.org/10.1038/s41893-023-01082-z.
25. Zhang, S., Hu, Q., Zhang, Y.X., Guo, H., Wu, Y., Sun, M., Zhu, X., Zhang, J., Gong, S., Liu, P., and Niu, Z. (2023). Depolymerization of polyesters by a binuclear catalyst for plastic recycling. Nat. Sustain. *6*, 965–973. https://doi.org/10.1038/s41893-023-01118-4.
26. Leng, Z., Padhan, R.K., and Sreeram, A. (2018). Production of a sustainable paving material through chemical recycling of waste PET into crumb rubber modified asphalt. J. Clean. Prod. *180*, 682–688. https://doi.org/10.1016/j.jclepro.2018.01.171.
27. Barnard, E., Rubio Arias, J.J., and Thielemans, W. (2021). Chemolytic depolymerisation of PET: a review. Green Chem. *23*, 3765–3789. https://doi.org/10.1039/d1gc00887k.
28. Sinha, V., Patel, M.R., and Patel, J.V. (2010). PET waste management by chemical recycling: a review. J. Polym. Environ. *18*, 8–25. https://doi.org/10.1007/s10924-008-0106-7.
29. Kaiho, S., Hmayed, A.A.R., Delle Chiaie, K.R., Worch, J.C., and Dove, A.P. (2022). Designing Thermally Stable Organocatalysts for Poly(ethylene terephthalate) Synthesis: Toward a One-Pot, Closed-Loop Chemical Recycling System for PET. Macromolecules *55*, 10628–10639. https://doi.org/10.1021/acs.macromol.2c01410.
30. Tan, M.Y., Goh, L., Safanama, D., Loh, W.W., Ding, N., Chien, S.W., Goh, S.S., Thitsartarn, W., Lim, J.Y.C., and Fam, D.W.H. (2022). Upcycling waste poly (ethylene terephthalate) into polymer electrolytes. J. Mater. Chem. A Mater. *10*, 24468–24474.
31. Yue, Q., Wang, C., Zhang, L., Ni, Y., and Jin, Y. (2011). Glycolysis of poly (ethylene terephthalate)(PET) using basic ionic liquids as catalysts. Polym. Degrad. Stabil. *96*, 399–403.
32. Jehanno, C., Pe´rez-Madrigal, M.M., Demarteau, J., Sardon, H., and Dove, A.P. (2019). Organocatalysis for depolymerisation. Polym. Chem. *10*, 172–186.
33. Vedage, G., Herman, R.G., and Klier, K. (1985). Chemical trapping of surface intermediates in methanol synthesis by amines. J. Catal. *95*, 423–434. https://doi.org/10.1016/0021-9517(85)90120-4.
34. Bao, Y.-S., Zhaorigetu, B., Agula, B., Baiyin, M., and Jia, M. (2014). Aminolysis of Aryl Ester Using Tertiary Amine as Amino Donor via C–O and C–N Bond Activations. J. Org. Chem. *79*, 803–808.
35. Allen, R.D., Bajjuri, K.M., Hedrick, J.L., Breyta, G., and Larson, C.E. (2016). Methods and Materials for Depolymerizing Polyesters.
36. Hofmann, M., Sundermeier, J., Alberti, C., and Enthaler, S. (2020). Zinc (II) acetate catalyzed depolymerization of poly (ethylene terephthalate). ChemistrySelect *5*, 10010–10014.

37. Shi, C., Quinn, E.C., Diment, W.T., and Chen, E.Y.-X. (2024). Recyclable and (Bio) degradable Polyesters in a Circular Plastics Economy. Chem. Rev. *124*, 4393–4478.

38. Peez, N., Becker, J., Ehlers, S.M., Fritz, M., Fischer, C.B., Koop, J.H.E., Winkelmann, C., and Imhof, W. (2019). Quantitative analysis of PET microplastics in environmental model samples using quantitative ^{1}H-NMR spectroscopy: validation of an optimized and consistent sample clean-up method. Anal. Bioanal. Chem. *411*, 7409–7418. https://doi.org/10.1007/s00216-019-02089-2.

39. Bartolome, L., Imran, M., Cho, B.G., Al-Masry, W.A., and Kim, D.H. (2012). Recent Developments in the Chemical Recycling of PET.

40. Karst, D., and Yang, Y. (2005). Using the solubility parameter to explain disperse dye sorption on polylactide. J. Appl. Polym. Sci. *96*, 416–422. https://doi.org/10.1002/app.21456.

41. Jaegers, N.R., Mueller, K.T., Wang, Y., and Hu, J.Z. (2020). Variable temperature and pressure operando MAS NMR for catalysis science and related materials. Acc. Chem. Res. *53*, 611–619. https://doi.org/10.1021/acs.accounts.9b00557.

42. Jaegers, N.R., Hu, W., Wang, Y., and Hu, J.Z. (2020). High-temperature and high-pressure in situ magic angle spinning nuclear magnetic resonance spectroscopy. JoVE *164*, e61794. https://doi.org/10.3791/61794.

43. Kim, D.H., Han, D.O., In Shim, K., Kim, J.K., Pelton, J.G., Ryu, M.H., Joo, J.C., Han, J.W., Kim, H.T., and Kim, K.H. (2021). One-pot chemo-bioprocess of PET depolymerization and recycling enabled by a biocompatible catalyst, betaine. ACS Catal. *11*, 3996–4008. https://doi.org/10.1021/acscatal.0c04014.

44. Pham, D.D., and Cho, J. (2021). Low-energy catalytic methanolysis of poly (ethyleneterephthalate). Green Chem. *23*, 511–525.

45. Genta, M., Goto, M., and Sasaki, M. (2010). Heterogeneous continuous kinetics modeling of PET depolymerization in supercritical methanol. J. Supercrit. Fluids *52*, 266–275.

46. Jaegers, N.R., Wang, Y., and Hu, J.Z. (2020). Thermal perturbation of NMR properties in small polar and non-polar molecules. Sci. Rep. *10*, 6097–6099. https://doi.org/10.1038/s41598-020-63174-6.

47. Becke, A.D. (1988). Density-functional exchange-energy approximation with correct asymptotic behavior. Phys. Rev. *38*, 3098–3100. https://doi.org/10.1103/physreva.38.3098.

48. Lee, C., Yang, W., and Parr, R.G. (1988). Development of the Colle-Salvetti correlation-energy formula into a functional of the electron density. Phys. Rev. B *37*, 785–789. https://doi.org/10.1103/PhysRevB.37.785.

49. Van Lenthe, E., and Baerends, E.J. (2003). Optimized Slater-type basis sets for the elements 1–118. J. Comput. Chem. *24*, 1142–1156. https://doi.org/10.1002/jcc.10255.

50. Hu, W., Jaegers, N.R., Winkelman, A.D., Murali, S., Mueller, K.T., Wang, Y., and Hu, J.Z. (2022). Modelling complex molecular interactions in catalytic materials for energy storage and conversion in nuclear magnetic resonance. Front. Catal. *2*, 935174. https://doi.org/10.3389/fctls.2022.935174.

51. Hu, J.Z., Jaegers, N.R., Hahn, N.T., Hu, W., Han, K.S., Chen, Y., Sears, J.A., Murugesan, V., Zavadil, K.R., and Mueller, K.T. (2022). Understanding the solvation-dependent properties of cyclic ether multivalent electrolytes using high-field NMR and quantum chemistry. JACS Au *2*, 917–932. https://doi.org/10.1021/jacsau.2c00046.

52. Kresse, G., and Furthmu¨ ller, J. (1996). Efficiency of ab-initio total energy calculations for metals and semiconductors using a plane-wave basis set. Comput. Mater. Sci. *6*, 15–50. https://doi.org/10.1016/0927-0256(96)00008-0.

53. Kresse, G., and Furthmu¨ ller, J. (1996). Efficient iterative schemes for ab initio total-energy calculations using a plane-wave basis set. Phys. Rev. B *54*, 11169–11186. https://doi.org/10.1103/PhysRevB.54.11169.

54. Blo¨ chl, P.E. (1994). Projector augmented-wave method. Phys. Rev. B *50*, 17953–17979. https://doi.org/10.1103/PhysRevB.50.17953.

55. Perdew, J.P., Burke, K., and Ernzerhof, M. (1996). Generalized gradient approximation made simple. Phys. Rev. Lett. *77*, 3865–3868. https://doi.org/10.1103/PhysRevLett.77.3865.

56. Grimme, S., Antony, J., Ehrlich, S., and Krieg, H. (2010). A consistent and accurate ab initio parametrization of density functional dispersion correction (DFT-D) for the 94 elements H-Pu. J. Chem. Phys. *132*, 154104. https://doi.org/10.1063/1.3382344.

57. Nose´ , S. (1984). A molecular dynamics method for simulations in the canonical ensemble. Mol. Phys. *52*, 255–268. https://doi.org/10.1080/00268978400101201.

58. Hoover, W.G. (1985). Canonical dynamics: Equilibrium phase-space distributions. Phys. Rev. *31*, 1695–1697. https://doi.org/10.1103/physreva.31.1695.